Nasrin Ghanbari
OPTI 521 - Synopsis of a published Paper
November 5, 2012

Testing Aspheric Lenses: New Approaches

by W. Osten, B. D¨orband, E. Garbusi, Ch. Pruss, and L. Seifert
Published in 2010

Introduction

Aspheric lenses are an important class of optical elements because they allow for correction of aberrations in optical systems. A problem of interest in optical design is to develop new approaches for fabrication and testing of aspheric elements. The two approaches for testing aspheric surfaces suggested in this paper are:

- Using an array of coherent point sources to generate many testing wavefronts [1-3]
- Using a diffractive element as a null-optic in a chromatic Fizeau interferometer [4]

Testing with Multiple Illumination Sources

The main challenges for interferometric testing of aspheres include: resolving the extremely high fringe density and reducing vignetting. A computer generated hologram (CGH) can be used in a null test to cancel the wavefront produced by the aspheric surface [5-7]. In this method each type of surface under test requires fabrication of a new CGH, which could be costly and time consuming. The first method proposed in this paper is based on a modified Twyman-Green interferometer shown in Figure 1.

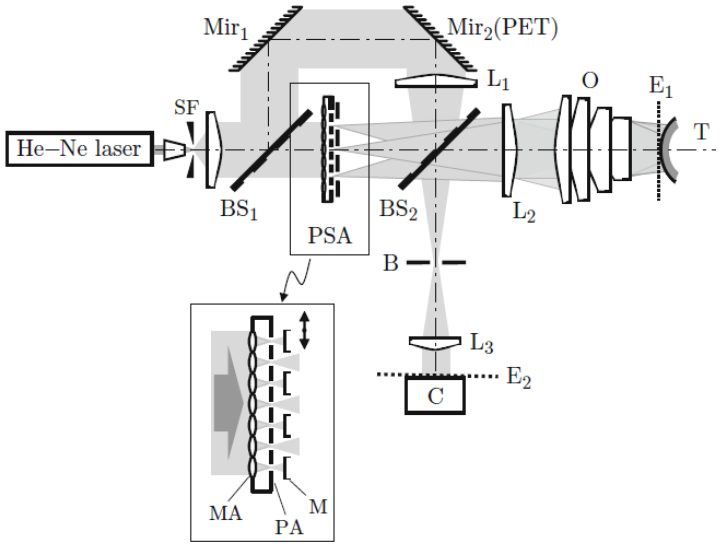

Figure 1. Experimental Setup

The test beam of the interferometer is incident on a diffractive optical element point source array (PSA) consisting of a microlens array (MA) and a pinhole array (PA) fabricated in a monolithic package. The PSA generates a two dimensional array of point sources and mask (M) moves over the array and select a particular set of points. Lens L_2 collimates these sources producing a set of wavefronts with different tilts. This set of wavefronts is reflected off of the aspheric element T and imaged by lens L_3 onto the detector C. The reference beam is focused by lens L_1 in the aperture B. This wavefront is then collimated by lens L_3 and combined with the test wavefront on the detector.

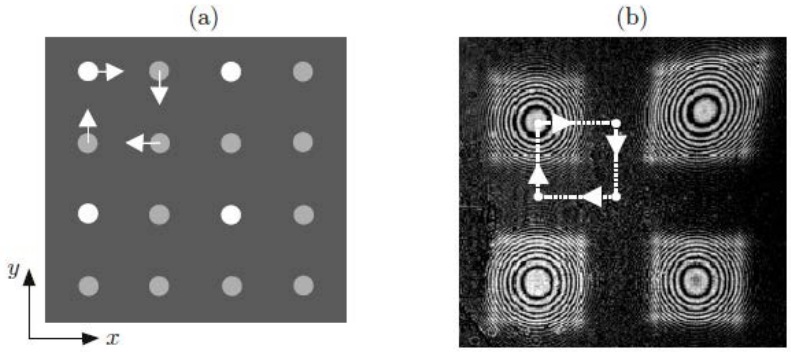

Figure 2. (a) Selection mask (M) moves over PSA in the x and y direction (sources indicated with white are active); (b) interferograms of active sources as seen on the camera

With this method the interferometer has to be calibrated in order to separate the contribution of the interferometer itself and the aspheric surface being tested. For each point source a reference sphere is placed in the test space; the position of the sphere is adjusted to obtain the minimum number of fringes on the detector. This data is used in an optimization process to derive the parameters that describe the aberrations of the interferometer. To test an asphere surface, corrections are calculated for these parameters in order to match the measured phase on the detector.

The results for an asphere surface with deviation of 900 µm from its best fit sphere and 1 µm from its design description reveal measurement accuracy on the order of $\sim 0.13\lambda$ peak-to-valley (PV). To calibrate this measurement a reference sphere with an accuracy of $\lambda/20$ was used in 90 test space positions. The accuracy is limited by mechanical stability of the interferometer; the high frequency details of aspheric surface are not modeled by this method.

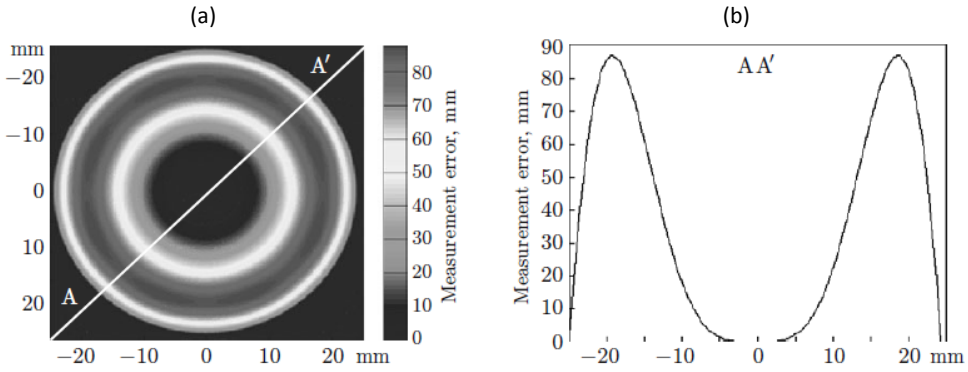

Figure 3. (a) The measurement error is approximately $\sim \mathbf{0.13}\boldsymbol{\lambda}$ PV; (b) Cut along the line AA'

Testing with Chromatic Fizeau Interferometer

With this method the authors propose using a tunable laser in a Fizeau interferometer to test aspheric elements. The setup is shown in Figure 4 with a diffractive optical element (DOE) as a null optic. Varying the laser wavelength changes the diffraction angle at the DOE and consequently the incident angle at the asphere. Each wavelength allows for measuring a different part of the asphere in the null test.

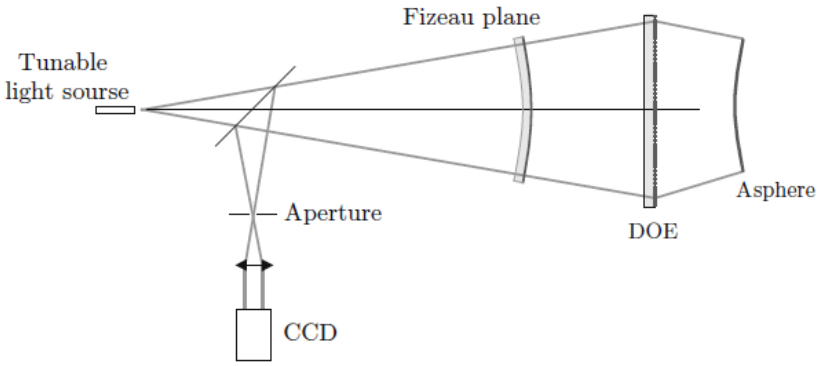

Figure 4. Chromatic Fizeau interferometer

To show the principle behind this method, the measurements of four aspheric surfaces are simulated. These aspheres have a potential application for the extreme ultra violate (EUV) lithography systems and they are all measured in the same setup. The parameters of this setup are adjusted such that the only variables are the wavelength and the distance between DOE and the asphere surface. A set of design constraints were put in place and a MATLAB program was implemented to determine solutions with the smallest measurement errors. The algorithm used for calculating measurement errors is shown in Figure 5. The ray tracing is done in ZEMAX and the diffraction orders up to the 20th order are included.

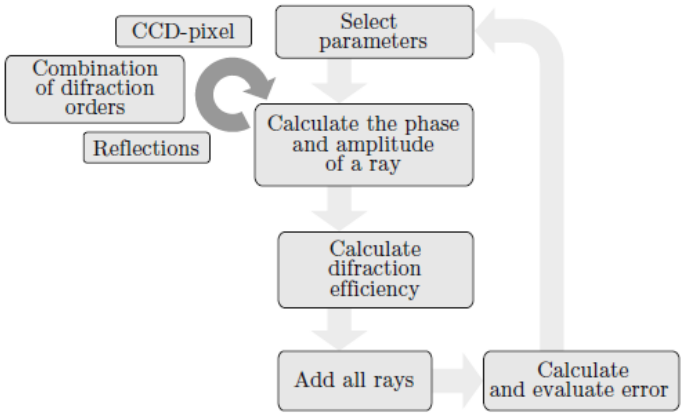

Figure 5. Diagram for optimization of measurement errors

Some of the constraints and simplifications in this simulation are:

- Cost of the DOE – to keep the cost down the line density is less than 550 line pairs per millimeter and the maximum diameter is less than 105 mm.

- Simulation of the aspheric form – to simplify the calculation the primary spherical aberration is used to simulate the aspheric form.

The number of measurements for each aspheric surface is determined by equation (1), where A is asphericity, λ is the central wavelength, and N is the maximum number of fringes allowed in each measurement [19]:

$$Number\ of\ measurements = \frac{64A}{3\lambda N} \tag{1}$$

The requirement for the detector is set by the minimum zone width which can be calculated with the number of pixels P over the aperture:

$$Minimal\ Zone = \frac{PN\lambda}{128A} \tag{2}$$

In testing each asphere the distance between the DOE and the asphere changes to accommodate for the size of the DOE. Concave aspheres are measured in minus one diffraction order. Convex aspheres are measured in plus one diffraction order on the way to the asphere and plus one order on the way back, (+1/+1). The drawback in this method is that other combinations of diffraction order are not completely blocked by the aperture and will disturb the measurement. For example the diffraction order (+1/+1) is disturbed by (+3/+3) at the wavelength of 820 µm as shown in Figure 6. To reduce this error the MATLAB program calculates and evaluates the error and changes the system parameters, this optimization process is shown in Figure 5.

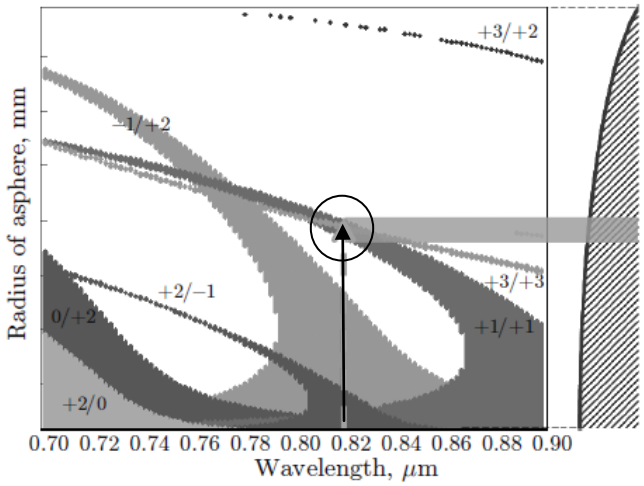

Figure 6. Combination of diffracted orders along the radius of an asphere; notice the distortion of the (+1/+1) measurement by the (+3/+3) order at 820 µm

Simulation Results

The distance from laser to DOE is set at 1100 mm and asphere No. 2 is placed in the test space at a distance of 333 mm from the DOE. Simulation of this case shows that the number of error sources increase near the optical axis. The varying intensity of different diffraction orders results in a non linear distribution of measurement error as a function of the number of unwanted diffraction orders, which is shown in Figure 7a. To correct for the large error near axis a small blocking aperture is placed on the optical axis, the improvement in the error distribution can be seen in Figure 7b. This error can also be mitigated by using a larger DOE or an iterative algorithm that removes the disturbance computationally.

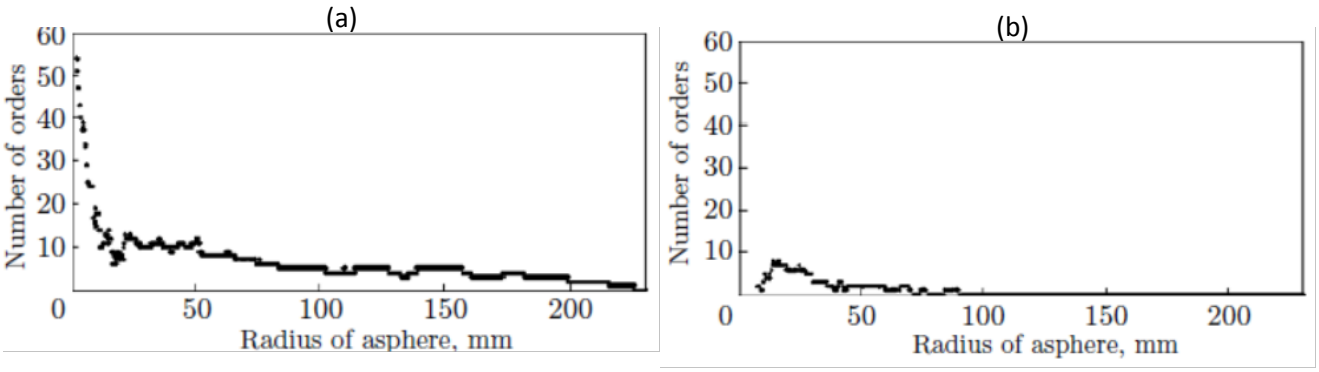

Figure 7. (a) Distribution of unwanted diffraction order along the radius; (b) Distribution of unwanted diffraction order along the radius after using a small blocking aperture on the optical axis

Table 1 lists the position of each of the four aspheres from the DOE along with the lateral resolution using a 4 megapixel camera, the wavelength range, and the central radius.

Table 1. Parameters for measurement of four EUV aspheres

Asphere number	Distance between DOE and asphere, mm	Image radius, mm	Lateral resolution (aperture diameter $d = 3.5$ mm), mm/pixel	Wavelength range, nm	Not evaluable central radius, mm
1	25.0	7.1	0.29	744–770	3
2	333.0	7.0	0.70	788–880	3
3	40.0	3.8	0.28	774–733	4
4	282.5	5.0	0.64	754–782	10

Conclusions

In this paper two methods were proposed for testing aspheres. In the first method, the aspheric surface was illuminated with an array of point sources in an interferometer. The advantage of this method is that, once the interferometer is calibrated, the aspheric surface measurements can be made extremely fast. The second method proposed is a chromatic Fizeau interferometer which is only simulated in this paper. This method offers flexibility as there are no moving parts, and it has been shown that four aspheres can easily be tested by adjusting the distance of the asphere relative to the DOE in the setup.

References

1. E. Garbusi, C. Pruss, J. Liesener, and W. Osten, "New Technique for Flexible and Rapid Measurement of Precision Aspheres," Proc. SPIE **6616**, 661629-1–661629-11 (2007).
2. C. Pruss, E. Garbusi, and W. Osten, "Testing Aspheres," Opt. Photon. News **19** (4), 24–29 (2008).
3. E. Garbusi, C. Pruss, and W. Osten, "Novel Interferometer for Precise and Flexible Asphere Testing," Opt. Lett. **33** (24), 2973–2975 (2009).
4. L. Seifert, C. Pruss, B. Dörband, and W. Osten, "Measuring Aspheres with a Chromatic Fizeau Interferometer," Proc. SPIE **7389**, 738919-1–738919-9 (2009).
5. J. C. Wyant and P. K. O'Neill, "Computer Generated Holograms: Null Lens Test of Aspheric Wave-Fronts," Appl. Opt. **13** (12), 2762–2765 (1974).

6. C. Pruss, S. Reichelt, H. J. Tiziani, and W. Osten, "Computer-Generated Holograms in Interferometric Testing," Opt. Eng. **43** (11), 2534–2540 (2004).
7. A. G. Poleshchuk, V. P. Korol'kov, V. V. Cherkashin, S. Reichelt, and J. Burge, "Methods for Minimizing the Errors in Direct Laser Writing of Diffractive Optical Elements," Avtometriya **38** (3), 3–19 (2002) [Optoelectr., Instrum. Data Process. **38** (3), 3–15 (2002)].

19. L. Seifert, Flexible Verfahren zur Vermessung asphärischer Flächen, PhD Thesis. (Univ. Stuttgart, Stuttgart, 2009).